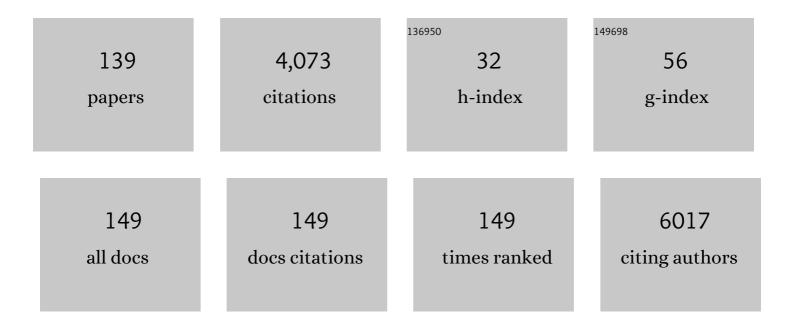
Winnok H De Vos

List of Publications by Year in descending order

Source: https://exaly.com/author-pdf/7641186/publications.pdf Version: 2024-02-01



#	Article	IF	CITATIONS
1	Repetitive disruptions of the nuclear envelope invoke temporary loss of cellular compartmentalization in laminopathies. Human Molecular Genetics, 2011, 20, 4175-4186.	2.9	250
2	Edible applications of shellac oleogels: spreads, chocolate paste and cakes. Food and Function, 2014, 5, 645-652.	4.6	204
3	Photothermal nanofibres enable safe engineering of therapeutic cells. Nature Nanotechnology, 2021, 16, 1281-1291.	31.5	192
4	Biopolymer-Based Structuring of Liquid Oil into Soft Solids and Oleogels Using Water-Continuous Emulsions as Templates. Langmuir, 2015, 31, 2065-2073.	3.5	156
5	Preparation and rheological characterization of shellac oleogels and oleogel-based emulsions. Journal of Colloid and Interface Science, 2013, 411, 114-121.	9.4	143
6	Transcriptional analysis through RNA sequencing of giant cells induced by Meloidogyne graminicola in rice roots. Journal of Experimental Botany, 2013, 64, 3885-3898.	4.8	128
7	Sustained synchronized neuronal network activity in a human astrocyte co-culture system. Scientific Reports, 2016, 6, 36529.	3.3	120
8	Exploring real-time in vivo redox biology of developing and aging Caenorhabditis elegans. Free Radical Biology and Medicine, 2012, 52, 850-859.	2.9	113
9	The Auxin-Regulated CrRLK1L Kinase ERULUS Controls Cell Wall Composition during Root Hair Tip Growth. Current Biology, 2018, 28, 722-732.e6.	3.9	113
10	Shellac as a natural material to structure a liquid oil-based thermo reversible soft matter system. RSC Advances, 2013, 3, 5324.	3.6	83
11	Novel cellulose and polyamide halochromic textile sensors based on the encapsulation of Methyl Red into a sol–gel matrix. Sensors and Actuators B: Chemical, 2012, 162, 27-34.	7.8	81
12	High-throughput fabrication of vascularized spheroids for bioprinting. Biofabrication, 2018, 10, 035009.	7.1	80
13	Early pathologic amyloid induces hypersynchrony of BOLD restingâ€state networks in transgenic mice and provides an early therapeutic window before amyloid plaque deposition. Alzheimer's and Dementia, 2016, 12, 964-976.	0.8	76
14	In silico synchronization reveals regulators of nuclear ruptures in lamin A/C deficient model cells. Scientific Reports, 2016, 6, 30325.	3.3	74
15	Untargeted metabolomics of colonic digests reveals kynurenine pathway metabolites, dityrosine and 3-dehydroxycarnitine as red versus white meat discriminating metabolites. Scientific Reports, 2017, 7, 42514.	3.3	71
16	Increased plasticity of the nuclear envelope and hypermobility of telomeres due to the loss of A–type lamins. Biochimica Et Biophysica Acta - General Subjects, 2010, 1800, 448-458.	2.4	65
17	Sustained accumulation of prelamin A and depletion of lamin A/C both cause oxidative stress and mitochondrial dysfunction but induce different cell fates. Nucleus, 2015, 6, 236-246.	2.2	63
18	Auranofin reveals therapeutic anticancer potential by triggering distinct molecular cell death mechanisms and innate immunity in mutant p53 non-small cell lung cancer. Redox Biology, 2021, 42, 101949.	9.0	63

#	Article	IF	CITATIONS
19	Cell monolayers sense curvature by exploiting active mechanics and nuclear mechanoadaptation. Nature Physics, 2021, 17, 1382-1390.	16.7	54
20	Lamins as mediators of oxidative stress. Biochemical and Biophysical Research Communications, 2012, 421, 635-639.	2.1	53
21	Interaction of the Tobacco Lectin with Histone Proteins Â. Plant Physiology, 2011, 155, 1091-1102.	4.8	47
22	Radiation-induced alternative transcription and splicing events and their applicability to practical biodosimetry. Scientific Reports, 2016, 6, 19251.	3.3	47
23	Controlled light exposure microscopy reveals dynamic telomere microterritories throughout the cell cycle. Cytometry Part A: the Journal of the International Society for Analytical Cytology, 2009, 75A, 428-439.	1.5	46
24	Synergetic effect of electrospun PCL fiber size, orientation and plasma-modified surface chemistry on stem cell behavior. Applied Surface Science, 2019, 485, 204-221.	6.1	46
25	Vapor nanobubble is the more reliable photothermal mechanism for inducing endosomal escape of siRNA without disturbing cell homeostasis. Journal of Controlled Release, 2020, 319, 262-275.	9.9	45
26	Guar and xanthan gum differentially affect shear induced breakdown of native waxy maize starch. Food Hydrocolloids, 2014, 35, 546-556.	10.7	44
27	High content image cytometry in the context of subnuclear organization. Cytometry Part A: the Journal of the International Society for Analytical Cytology, 2010, 77A, 64-75.	1.5	42
28	Fast spatial-selective delivery into live cells. Journal of Controlled Release, 2017, 266, 198-204.	9.9	40
29	Gums tuning the rheological properties of modified maize starch pastes: Differences between guar and xanthan. Food Hydrocolloids, 2014, 39, 85-94.	10.7	38
30	Loss of Nuclear Envelope Integrity in Aging and Disease. International Review of Cell and Molecular Biology, 2018, 336, 205-222.	3.2	38
31	Differential response to acute low dose radiation in primary and immortalized endothelial cells. International Journal of Radiation Biology, 2013, 89, 841-850.	1.8	36
32	Reducing Compounds Equivocally Influence Oxidation during Digestion of a High-Fat Beef Product, which Promotes Cytotoxicity in Colorectal Carcinoma Cell Lines. Journal of Agricultural and Food Chemistry, 2016, 64, 1600-1609.	5.2	36
33	Chronic exposure to simulated space conditions predominantly affects cytoskeleton remodeling and oxidative stress response in mouse fetal fibroblasts. International Journal of Molecular Medicine, 2014, 34, 606-615.	4.0	35
34	Gene expression-based biodosimetry for radiological incidents: assessment of dose and time after radiation exposure. International Journal of Radiation Biology, 2019, 95, 64-75.	1.8	34
35	Profilin-I-ligand interactions influence various aspects of neuronal differentiation. Journal of Cell Science, 2006, 119, 1570-1578.	2.0	33
36	Different replication characteristics of historical pseudorabies virus strains in porcine respiratory nasal mucosa explants. Veterinary Microbiology, 2009, 136, 341-346.	1.9	33

#	Article	IF	CITATIONS
37	MorphoNeuroNet: An automated method for dense neurite network analysis. Cytometry Part A: the Journal of the International Society for Analytical Cytology, 2014, 85, 188-199.	1.5	33
38	Comparative analysis reveals Ce3D as optimal clearing method for in toto imaging of the mouse intestine. Neurogastroenterology and Motility, 2019, 31, e13560.	3.0	32
39	Chemogenetic silencing of neurons in the mouse anterior cingulate area modulates neuronal activity and functional connectivity. NeuroImage, 2020, 220, 117088.	4.2	32
40	Image-Based Profiling of Synaptic Connectivity in Primary Neuronal Cell Culture. Frontiers in Neuroscience, 2018, 12, 389.	2.8	30
41	Regional vulnerability and spreading of hyperphosphorylated tau in seeded mouse brain. Neurobiology of Disease, 2019, 127, 398-409.	4.4	30
42	Microbial community of predatory bugs of the genus Macrolophus(Hemiptera: Miridae). BMC Microbiology, 2012, 12, S9.	3.3	29
43	Targeted Perturbation of Nuclear Envelope Integrity with Vapor Nanobubble-Mediated Photoporation. ACS Nano, 2018, 12, 7791-7802.	14.6	29
44	Simulated microgravity decreases apoptosis in fetal fibroblasts. International Journal of Molecular Medicine, 2012, 30, 309-313.	4.0	27
45	Induced pluripotent stem cell-derived motor neurons of CMT type 2 patients reveal progressive mitochondrial dysfunction. Brain, 2021, 144, 2471-2485.	7.6	27
46	Medium-mediated DNA repair response after ionizing radiation is correlated with the increase of specific cytokines in human fibroblasts. Mutation Research - Fundamental and Molecular Mechanisms of Mutagenesis, 2010, 687, 40-48.	1.0	26
47	Combined Consumption of Beefâ€Based Cooked Mince and Sucrose Stimulates Oxidative Stress, Cardiac Hypertrophy, and Colonic Outgrowth of Desulfovibrionaceae in Rats. Molecular Nutrition and Food Research, 2019, 63, e1800962.	3.3	25
48	Cytoplasmic localization of PML particles in laminopathies. Histochemistry and Cell Biology, 2013, 139, 119-134.	1.7	24
49	Invited Review Article: Advanced light microscopy for biological space research. Review of Scientific Instruments, 2014, 85, 101101.	1.3	24
50	Procaine Induces Cytokinesis in Horse Oocytes via a pH-Dependent Mechanism1. Biology of Reproduction, 2015, 93, 23.	2.7	24
51	Follicles of various maturation stages react differently to enzymatic isolation: a comparison of different isolation protocols. Reproductive BioMedicine Online, 2015, 30, 181-190.	2.4	23
52	Deregulation of focal adhesion formation and cytoskeletal tension due to loss of A-type lamins. Cell Adhesion and Migration, 2017, 11, 447-463.	2.7	23
53	Selective Labeling of Individual Neurons in Dense Cultured Networks With Nanoparticle-Enhanced Photoporation. Frontiers in Cellular Neuroscience, 2018, 12, 80.	3.7	23
54	Validated comprehensive metabolomics and lipidomics analysis of colon tissue and cell lines. Analytica Chimica Acta, 2019, 1066, 79-92.	5.4	23

#	Article	IF	CITATIONS
55	Statins and Histone Deacetylase Inhibitors Affect Lamin A/C – Histone Deacetylase 2 Interaction in Human Cells. Frontiers in Cell and Developmental Biology, 2019, 7, 6.	3.7	23
56	In vivo interaction between the tobacco lectin and the core histone proteins. Journal of Plant Physiology, 2014, 171, 1149-1156.	3.5	22
57	Systematic Quantification of Synapses in Primary Neuronal Culture. IScience, 2020, 23, 101542.	4.1	22
58	Polydopamine–Gelatin as Universal Cell-Interactive Coating for Methacrylate-Based Medical Device Packaging Materials: When Surface Chemistry Overrules Substrate Bulk Properties. Biomacromolecules, 2016, 17, 56-68.	5.4	21
59	Internalization of <i>Sambucus nigra</i> agglutinins I and II in insect midgut CFâ€203 cells. Archives of Insect Biochemistry and Physiology, 2011, 76, 211-222.	1.5	20
60	Mechanism of entomotoxicity of the plant lectin from Hippeastrum hybrid (Amaryllis) in Spodoptera littoralis larvae. Journal of Insect Physiology, 2012, 58, 1177-1183.	2.0	20
61	Sperm involved in recurrent partial hydatidiform moles cannot induce the normal pattern of calcium oscillations. Fertility and Sterility, 2014, 102, 581-588.e1.	1.0	20
62	A multilevel framework to reconstruct anatomical 3D models of the hepatic vasculature in rat livers. Journal of Anatomy, 2017, 230, 471-483.	1.5	20
63	High Content Analysis of Human Fibroblast Cell Cultures after Exposure to Space Radiation. Radiation Research, 2009, 172, 423-436.	1.5	19
64	Gold nanodome-patterned microchips for intracellular surface-enhanced Raman spectroscopy. Analyst, The, 2015, 140, 8080-8087.	3.5	19
65	Dysregulation of Microtubule Stability Impairs Morphofunctional Connectivity in Primary Neuronal Networks. Frontiers in Cellular Neuroscience, 2017, 11, 173.	3.7	19
66	Modulation of gene expression in endothelial cells in response to high LET nickel ion irradiation. International Journal of Molecular Medicine, 2014, 34, 1124-1132.	4.0	17
67	Quantitative analysis of hepatic macro―and microvascular alterations during cirrhogenesis in theÂrat. Journal of Anatomy, 2018, 232, 485-496.	1.5	17
68	2D mapping of strongly deformable cell nucleiâ€based on contour matching. Cytometry Part A: the Journal of the International Society for Analytical Cytology, 2011, 79A, 580-588.	1.5	16
69	Oral microbiota reduce wound healing capacity of epithelial monolayers, irrespective of the presence of 5-fluorouracil. Experimental Biology and Medicine, 2018, 243, 350-360.	2.4	15
70	High-throughput microscopy exposes a pharmacological window in which dual leucine zipper kinase inhibition preserves neuronal network connectivity. Acta Neuropathologica Communications, 2019, 7, 93.	5.2	15
71	Two novel techniques to detect follicles in human ovarian cortical tissue. Human Reproduction, 2006, 21, 1720-1724.	0.9	14
72	Repeated exposure of human fibroblasts to ionizing radiation reveals an adaptive response that is not mediated by interleukin-6 or TGF-1². Mutation Research - Fundamental and Molecular Mechanisms of Mutagenesis, 2011, 715, 19-24.	1.0	14

#	Article	IF	CITATIONS
73	Mitochondrial efficiency is increased in axenically cultured Caenorhabditis elegans. Experimental Gerontology, 2014, 56, 26-36.	2.8	14
74	Intracellular pH Response to Weak Acid Stress in Individual Vegetative Bacillus subtilis Cells. Applied and Environmental Microbiology, 2016, 82, 6463-6471.	3.1	14
75	Long-term live-cell microscopy with labeled nanobodies delivered by laser-induced photoporation. Nano Research, 2020, 13, 485-495.	10.4	14
76	Screening of soy and milk protein hydrolysates for their ability to activate the CCK1 receptor. Peptides, 2012, 34, 226-231.	2.4	13
77	Focus on Bio-Image Informatics. Advances in Anatomy, Embryology and Cell Biology, 2016, , .	1.6	13
78	Strontium fails to induce Ca2+ release and activation in human oocytes despite the presence of functional TRPV3 channels. Human Reproduction Open, 2018, 2018, hoy005.	5.4	13
79	Caenorhabditis elegans as a Model System for Studying Drug Induced Mitochondrial Toxicity. PLoS ONE, 2015, 10, e0126220.	2.5	12
80	Integrated High-Content Quantification of Intracellular ROS Levels and Mitochondrial Morphofunction. Advances in Anatomy, Embryology and Cell Biology, 2016, 219, 149-177.	1.6	12
81	Minimal processing of iceberg lettuce has no substantial influence on the survival, attachment and internalization of E. coli O157 and Salmonella. International Journal of Food Microbiology, 2016, 238, 40-49.	4.7	12
82	Bypassing Border Control: Nuclear Envelope Rupture in Disease. Physiology, 2018, 33, 39-49.	3.1	12
83	Fourâ€dimensional telomere analysis in recordings of living human cells acquired with Controlled Light Exposure Microscopy. Journal of Microscopy, 2010, 238, 254-264.	1.8	11
84	Monitoring the intracellular pH of Zygosaccharomyces bailii by green fluorescent protein. International Journal of Food Microbiology, 2012, 156, 290-295.	4.7	11
85	Effects of metformin on tumor hypoxia and radiotherapy efficacy: a [18F]HX4 PET imaging study in colorectal cancer xenografts. EJNMMI Research, 2019, 9, 74.	2.5	11
86	Hypersynchronicity in the default mode-like network in a neurodevelopmental animal model with relevance for schizophrenia. Behavioural Brain Research, 2019, 364, 303-316.	2.2	11
87	Time-resolved quantitative analysis of CCK1 receptor-induced intracellular calcium increase. Peptides, 2012, 34, 219-225.	2.4	10
88	Selective Glucocorticoid Receptor Properties of GSK866 Analogs with Cysteine Reactive Warheads. Frontiers in Immunology, 2017, 8, 1324.	4.8	10
89	Analysis of Polymorphic Membrane Protein Expression in Cultured Cells Identifies PmpA and PmpH of Chlamydia psittaci as Candidate Factors in Pathogenesis and Immunity to Infection. PLoS ONE, 2016, 11, e0162392.	2.5	10
90	Accurate Detection of Dysmorphic Nuclei Using Dynamic Programming and Supervised Classification. PLoS ONE, 2017, 12, e0170688.	2.5	10

#	Article	IF	CITATIONS
91	Prediction of biological age by morphological staging of sarcopenia in <i>Caenorhabditis elegans</i> . DMM Disease Models and Mechanisms, 2021, 14, .	2.4	10
92	The cellular response to plasma membrane disruption for nanomaterial delivery. Nano Convergence, 2022, 9, 6.	12.1	10
93	The Cytotoxicity of Elderberry Ribosome-Inactivating Proteins Is Not Solely Determined by Their Protein Translation Inhibition Activity. PLoS ONE, 2015, 10, e0132389.	2.5	9
94	Probing cytoskeletal pre-stress and nuclear mechanics in endothelial cells with spatiotemporally controlled (de-)adhesion kinetics on micropatterned substrates. Cell Adhesion and Migration, 2017, 11, 98-109.	2.7	9
95	Immune remodelling of stromal cell grafts in the central nervous system: therapeutic inflammation or (harmless) side-effect?. Journal of Tissue Engineering and Regenerative Medicine, 2017, 11, 2846-2852.	2.7	9
96	Quantifying the growth of <i>chlamydia suis</i> in cell culture using high ontent microscopy. Microscopy Research and Technique, 2017, 80, 350-356.	2.2	9
97	Patients with a high proportion of immature and meiotically resistant oocytes experience defective nuclear oocyte maturation patterns and impaired pregnancy outcomes. Reproductive BioMedicine Online, 2018, 36, 396-407.	2.4	9
98	Progressive tau aggregation does not alter functional brain network connectivity in seeded hTau.P301L mice. Neurobiology of Disease, 2020, 143, 105011.	4.4	9
99	Rosiglitazone Protects Endothelial Cells From Irradiation-Induced Mitochondrial Dysfunction. Frontiers in Pharmacology, 2020, 11, 268.	3.5	9
100	Measurement of S-phase duration of adult stem cells in the flatwormMacrostomum lignanoby double replication labelling and quantitative colocalization analysis. Cell Biology International, 2012, 36, 1251-1259.	3.0	8
101	Inhibition of Transforming Growth Factor Î ² Signaling Promotes Epiblast Formation in Mouse Embryos. Stem Cells and Development, 2015, 24, 497-506.	2.1	8
102	Single-Cell and Neuronal Network Alterations in an In Vitro Model of Fragile X Syndrome. Cerebral Cortex, 2020, 30, 31-46.	2.9	8
103	Confined no more: Viral mechanisms of nuclear entry and egress. International Journal of Biochemistry and Cell Biology, 2020, 129, 105875.	2.8	8
104	Multiplexed profiling of secreted proteins for the detection of potential space biomarkers. Molecular Medicine Reports, 2011, 4, 17-23.	2.4	7
105	High-LET Carbon and Iron Ions Elicit a Prolonged and Amplified p53 Signaling and Inflammatory Response Compared to low-LET X-Rays in Human Peripheral Blood Mononuclear Cells. Frontiers in Oncology, 2021, 11, 768493.	2.8	7
106	SliceMap: an algorithm for automated brain region annotation. Bioinformatics, 2018, 34, 718-720.	4.1	6
107	Single cell epigenetic visualization assay. Nucleic Acids Research, 2021, 49, e43-e43.	14.5	6
108	Untargeted Metabolomics Reveals Elevated Lâ€Carnitine Metabolism in Pig and Rat Colon Tissue Following Red Versus White Meat Intake. Molecular Nutrition and Food Research, 2021, 65, e2000463.	3.3	6

#	Article	IF	CITATIONS
109	MYCN-induced nucleolar stress drives an early senescence-like transcriptional program in hTERT-immortalized RPE cells. Scientific Reports, 2021, 11, 14454.	3.3	6
110	Image Informatics Strategies for Deciphering Neuronal Network Connectivity. Advances in Anatomy, Embryology and Cell Biology, 2016, 219, 123-148.	1.6	5
111	Comprehensive polar metabolomics and lipidomics profiling discriminates the transformed from the non-transformed state in colon tissue and cell lines. Scientific Reports, 2021, 11, 17249.	3.3	5
112	Cellular senescence in neuroblastoma. British Journal of Cancer, 2022, 126, 1529-1538.	6.4	5
113	Luminescent HumanÂiPSC-Derived Neurospheroids Enable Modeling of Neurotoxicity After Oxygen–glucose Deprivation. Neurotherapeutics, 2022, 19, 550-569.	4.4	5
114	X-irradiation induces cell death in fetal fibroblasts. International Journal of Molecular Medicine, 2012, 30, 114-8.	4.0	4
115	Cellular Redox Profiling Using High-content Microscopy. Journal of Visualized Experiments, 2017, , .	0.3	4
116	Transferrins Reduce Replication of Chlamydia suis in McCoy Cells. Pathogens, 2021, 10, 858.	2.8	4
117	In Vivo Visualization and Quantification of Mitochondrial Morphology in C. elegans. Methods in Molecular Biology, 2015, 1265, 367-377.	0.9	3
118	Maternal Benzophenone Exposure Impairs Hippocampus Development and Cognitive Function in Mouse Offspring. Advanced Science, 2021, 8, e2102686.	11.2	3
119	Transient nuclear lamin A/C accretion aids in recovery from vapor nanobubble-induced permeabilisation of the plasma membrane. Cellular and Molecular Life Sciences, 2022, 79, 23.	5.4	3
120	Morpho-functional comparison of differentiation protocols to create iPSC-derived cardiomyocytes. Biology Open, 2022, 11, .	1.2	3
121	Cells infected with human papilloma pseudovirus display nuclear reorganization and heterogenous infection kinetics. Cytometry Part A: the Journal of the International Society for Analytical Cytology, 0, , .	1.5	3
122	Identification of healthspan-promoting genes in Caenorhabditis elegans based on a human GWAS study. Biogerontology, 2022, 23, 431-452.	3.9	3
123	Response to low-dose X-irradiation is p53-dependent in a papillary thyroid carcinoma model system. International Journal of Oncology, 2011, 39, 1429-41.	3.3	2
124	BiDiFuse: a FIJI plugin for fusing bi-directionally recorded microscopic image volumes. Bioinformatics, 2016, 32, 3691-3693.	4.1	2
125	High-throughput Analysis of Synaptic Activity in Electrically Stimulated Neuronal Cultures. Neuroinformatics, 2021, 19, 737-750.	2.8	2
126	Fractionated irradiation of <scp>MCF7</scp> breast cancer cells rewires a gene regulatory circuit towards a treatmentâ€resistant stemness phenotype. Molecular Oncology, 2022, 16, 3410-3435.	4.6	2

#	Article	IF	CITATIONS
127	The AMERE project: Enabling real-time detection of radiation effects in individual cells in deep space. Planetary and Space Science, 2012, 74, 84-96.	1.7	1
128	In Vivo Visualization and Quantification of in C. elegans. Methods in Molecular Biology, 2021, 2276, 397-407.	0.9	1
129	VNB-mediated endosomal escape triggers robust gene silencing in human cell lines. , 2020, , .		1
130	High Content Image Cytometry. Imaging & Microscopy, 2009, 11, 46-48.	0.1	0
131	2D mapping of strongly deformed cell nuclei based on contour warping. , 2010, 2010, 4379-82.		0
132	Corrigendum to "Lamins as mediators of oxidative stress―[Biochem. Biophys. Res. Commun. 421 (2012) 635à€"639]. Biochemical and Biophysical Research Communications, 2012, 424, 201.	2.1	0
133	Nanodome coins for intracellular surface-enhanced Raman spectroscopy. , 2015, , .		0
134	Cell response of flexible PMMA-derivatives: supremacy of surface chemistry over substrate stiffness. Journal of Materials Science: Materials in Medicine, 2017, 28, 183.	3.6	0
135	Image informatics for studying the role of Alzheimer's disease-related toxic proteins on neuronal network connectivity in primary co-cultures Frontiers in Neuroinformatics, 0, 9, .	2.5	0
136	Accurate detection of dysmorphic nuclei in neuronal networks. Frontiers in Neuroinformatics, 0, 9, .	2.5	0
137	An in vitro toolbox to study synaptic connectivity in health and disease. Frontiers in Neuroscience, 0, 9, .	2.8	0
138	Molecular biochemical characterization of selective glucocorticoid receptor activities of GSK866 analogues with cysteine reactive warheads. Proceedings for Annual Meeting of the Japanese Pharmacological Society, 2018, WCP2018, PO2-5-6.	0.0	0
139	Comparison of different clearing protocols for <i>in toto</i> threeâ€dimensional microscopic imaging of the intestinal wall. FASEB Journal, 2018, 32, 642.2.	0.5	0